Journal of the American Heart Association

Check for updates

ORIGINAL RESEARCH

Risk Stratification of Patients With Type 2 Long-QT Syndrome Through Analysis of T-Wave Morphology

Neurys Gómez, MSc; Julia Ramírez, PhD; Aleksei A. Savelev, MD; Pia Dahlberg, MD, PhD; Anneli Svensson, MD, PhD; Nina Larsson, MD, PhD; Erik Ljungström, MD; Uzma Chaudhry, MD, PhD; Juan Pablo Martínez, PhD; Pablo Laguna, PhD*; Pyotr G. Platonov, MD, PhD*

BACKGROUND: Risk stratification in type 2 long-QT syndrome remains challenging, as QT duration may not fully reflect all underlying arrhythmic vulnerability. We assessed whether an index derived from the T-wave morphology is associated with cardiac events in a cohort with type 2 long-QT syndrome.

METHODS: We retrospectively and prospectively analyzed 54 genotype-confirmed patients with type 2 long-QT syndrome. T-wave morphology in 8 independent leads was assessed using a warping-based index, the T-wave morphology variation (TMV) index, quantifying T-wave morphologic changes from a general population-based reference T-wave. Association with the first lifetime occurrence of a cardiac event, including either syncope or the combined ventricular arrhythmia end point, was tested using univariate and multivariable Cox regression models.

RESULTS: Using the 25th-percentile threshold (TMV≤–18.41 ms), more negative TMV values indicating greater morphologic changes and a broader or delayed repolarization phase in the T-wave signal relative to the control, as observed in lead I, were significantly associated with increased risk of cardiac event (hazard ratio [HR], 3.505 [95% CI, 1.673–7.341]; $P<0.001$). The association remained significant after adjustment for corrected QT (HR, 2.92 [95% CI, 1.111–7.676]; $P=0.03$) and after additional adjustment for sex (HR, 3.375 [95% CI, 1.256–9.067]; $P=0.016$), and the T-wave morphology combination score (HR, 4.061 [95% CI, 1.369–12.046]; $P=0.012$).

CONCLUSIONS: T-wave morphology abnormalities, quantified using TMV, are associated with a higher risk of cardiac events after adjustment for corrected QT prolongation, sex, and morphology combination score. TMV could complement current risk stratification strategies, although confirmatory validation in larger, independent, prospective cohorts is pending.

Key Words: arrhythmic risk ■ cardiac events ■ long-QT syndrome ■ time warping ■ T-wave morphology

Downloaded from http://ahajournals.org by on July 6, 2026

Long-QT syndrome (LQTS) is an inherited channelopathy with an estimated prevalence of ≈1:2000, with a slight female predominance.[1,2] Type 2 long-QT syndrome (LQT2) is caused by pathogenic variants in the *KCNH2* gene and represents 1 of the most prevalent and clinically significant subtypes, accounting for up to 30% to 45% of genetically confirmed diagnoses.[3–5] It is characterized by disorders of myocardial repolarization that are associated with an increased propensity to atypical polymorphic ventricular tachycardia, called torsade de pointes,[6,7] which can manifest as syncopal episodes or lead to a sudden cardiac death.[4,6,7] The need to properly identify high-risk patients has prompted a growing body of research focused on improving risk prediction and early intervention.

Correspondence to: Neurys Gómez, University of Zaragoza Lab 6.1.01, C/ Mariano Esquillor s/n, CP: 50018, Zaragoza, Spain. Email: ngomez@unizar.es

*P. Laguna and P.G. Platonov are co–senior authors.

This manuscript was sent to Kevin F. Kwaku, MD, PhD, Associate Editor, for review by expert referees, editorial decision, and final disposition.

Supplemental Material is available at https://www.ahajournals.org/doi/suppl/10.1161/JAHA.125.048388

For Sources of Funding and Disclosures, see page 10.

© 2026 The Author(s). Published on behalf of the American Heart Association, Inc., by Wiley. This is an open access article under the terms of the Creative Commons Attribution-NonCommercial-NoDerivs License, which permits use and distribution in any medium, provided the original work is properly cited, the use is non-commercial and no modifications or adaptations are made.

JAHA is available at: www.ahajournals.org/journal/jaha

CLINICAL PERSPECTIVE

What is New?

- A novel index, T-wave morphology variation, provides, from a median heartbeat, quantification of T-wave morphology changes relative to a large-scale normal reference population.
- T-wave morphology variation is linked to a higher risk of cardiac events, maintaining this association after adjustment for sex, corrected QT prolongation, and the T-wave morphology combination score; T-wave amplitude and morphology combination score, considered individually, were not significantly associated with outcomes in this cohort.

What Are the Clinical Implications?

- This study is the first to provide evaluation of reference-based T-wave morphologic variations in patients with type 2 long-QT syndrome; T-wave morphology variation captures morphologic patterns that are significantly linked to cardiac events beyond corrected QT and may point to a future complementary role in risk stratification for patients with type 2 long-QT syndrome, including those with borderline or prolonged corrected QT values, pending validation in larger cohorts.

Nonstandard Abbreviations and Acronyms

CE	cardiac event
LQT2	type 2 long-QT syndrome
LQTS	long-QT syndrome
MCS	morphology combination score
QTc	corrected QT
T_{Amp}	T-wave amplitude
TMV	T-wave morphology variation
UKB	UK Biobank
VA	ventricular arrhythmia

LQT2 is primarily characterized by prolongation of the QT interval, which reflects the duration of myocardial repolarization.[8] Because the QT interval is strongly dependent on heart rate, it is commonly corrected for heart rate (corrected QT [QTc]), most often using the Bazett formula. QTc prolongation remains the pathophysiological hallmark for diagnostic and risk stratification.[8,9] However, ≈25% to 50% of genetically affected and asymptomatic individuals may present borderline or even normal QTc durations at rest,[10–12] underscoring the limitations of relying solely on the QTc interval for risk assessment. It has been pointed out that the proarrhythmic risk in LQT2 may not only stem from the delayed repolarization per se, but rather when associated with an increased temporal and spatial heterogeneity.[3,13] This view, supported by both experimental models and clinical observations,[13–16] has prompted the search for complementary markers capable of capturing the underlaying complexity of repolarization dynamics beyond what QTc duration alone can convey.

In LQT2, the resulting dysfunction of the rapid delayed rectifier potassium current[3] (I_{Kr}) leads to delayed ventricular repolarization, which manifests electrocardiographically as low-amplitude, asymmetric, notched, flattened, or bifid T waves.[16–18] Although these genotype-specific T-wave abnormalities are qualitatively recognized and may offer insights beyond QTc, they remain difficult to quantify and have not yet been systematically integrated into clinical risk stratification.[17] Clinically, the occurrence of arrhythmic events in LQT2 despite borderline or normal QTc[16] further draw attention to this gap and support the need for complementary approaches that capture the arrhythmogenic substrate beyond conventional QTc measurements.

Although several existing T-wave–based biomarkers aimed at enhancing risk stratification are commonly categorized as morphology-based markers for LQTS, most of them rely on temporal measurements derived from ECG fiducial points,[10,19–21] and therefore do not fully capture the morphologic complexity of the T wave. To overcome these limitations, biomarkers such as the morphology combination score (MCS)[22,23] and others, based on information provided by the vectorcardiogram, have been evaluated.[21,24] Separately, a time-warping–based index, d_w, was recently proposed to quantify pointwise time-domain variation between 2 distinct T waves by measuring the amount of warping required to align 1 T wave to another.[25] This method enables a more comprehensive, morphology-aware characterization of ventricular repolarization dispersion. Previous studies have demonstrated the value of d_w in capturing changes related to heart rate fluctuations (T-wave morphology restitution, TMR index)[26] in patients with heart failure[26] and in the general population,[27] and in ischemia-induced alterations through a version restricted to the T-peak-to-end interval in both human[28] and animal[29] models, as well as in an adapted d_w-based approach quantifying T-wave morphology variations (TMVs) with respect to a population-based reference T wave (TMV index),[30] which provides a global assessment of T-wave morphology and is the metric adopted in the present study. In this work, we hypothesized that a global assessment of T-wave morphology using TMV index may uncover relevant differences in repolarization dynamics beyond what conventional QT-based or fiducial-point–based markers can reveal. The aim of this study was to assess the association between the TMV

Downloaded from http://ahajournals.org by on July 6, 2026

index and the risk of cardiac events (CEs) in a cohort of patients with LQT2.

METHODS

Detailed methods are provided in Data S1. The data that support the findings of this study are available from the corresponding author on reasonable request.

Patient Cohort

The study population comprised individuals diagnosed with LQT2 recruited at the cardiogenetic clinics of the tertiary care academic hospitals in Lund, Gothenburg, and Linköping (Sweden). Inclusion criteria were patients (1) carrying a pathogenic or likely pathogenic genetic variant in *KCNH2* (LQT2), as confirmed by standard genetic testing according to clinical routines, and (2) at least 16 years old, to avoid potential variability in T-wave morphology typically observed in pediatric and adolescent populations. Patients with multiple LQTS-related genetic variants (>1) were not included in this study. Eight independent standard leads (I, II, and V1–V6) were collected during a 10-second resting recording in the supine position, and digital ECG files were exported from either GE MUSE ECG database (GE Healthcare, Chicago, IL) or Cardiolex ECG database (Cardiolex Medical AB, Solna, Sweden). Signals were acquired at a sampling frequency of 500 Hz and with an amplitude resolution of 4.88 μV. The earliest ECG ever recorded at or after the age of 16 years was used for analysis. The study received the Local Ethical Review Board approval 2024-05551-02 (Lund, Sweden), in accordance with national and international ethical and deontological standards.

The reference cohort consisted of 23 962 middle-aged adults with no history of cardiovascular disease, selected from the UK Biobank (UKB).[31] A reference library of normal T-wave morphologies, clustered by sex, heart rate, and lead, was previously derived from standard 10-second, 8-independent-lead resting ECGs available from the UKB database, as described by Ramírez et al.[30] Data access for this component of the study was granted under UKB application 8256. All participants provided informed consent, and the study received institutional ethics approval.

Data Collection and End Points

Study data corresponding to the first cohort (patients with LQT2) were collected and managed using Research Electronic Data Capture (REDCap) tools hosted at hospitals in Lund, Gothenburg, and Linköping (Sweden).[32,33] Clinical data included demographic information, ECG findings, ongoing treatments (including QT-prolonging medications), and clinical events documented both retrospectively (before inclusion into the registry) and prospectively throughout long-term follow-up. β-Blocker use was specifically collected to enable time-dependent analysis of its potential impact on cardiac outcomes.

The primary end point was defined as the first lifetime occurrence of a CE, defined as the occurrence of syncope (a sudden, transient loss of consciousness with rapid recovery) or the composite end point ventricular arrhythmia (VA). Accordingly, the first lifetime CE was ascertained from the complete medical record and could occur either before or after the first digital ECG used for TMV computation. Each patient contributed a single event time corresponding to the first lifetime CE. VA includes documented episodes of torsade de pointes, sustained ventricular tachycardia, appropriate intervention by an implantable cardioverter-defibrillator, aborted cardiac arrest (requiring external defibrillation), or LQTS-related sudden cardiac death (abrupt in onset and without an identifiable cause, whether witnessed or unwitnessed). VA was considered as a secondary end point.

ECG Signal Processing and Characterization

The ECG preprocessing pipeline for the clinical cohort with LQT2 comprised several stages. Initially, a bidirectional sixth-order Butterworth band-pass filter with a bandwidth of 0.5 to 40 Hz was applied to attenuate high-frequency noise, including electrical and muscular artifacts, and to minimize baseline wander. From each 10-second ECG recording, the median beat was extracted for each of the 8 independent leads (Figure 1A shows the median beat in lead I). QRS and T-wave onset and end timings were then annotated using a wavelet-based delineation method.[34] To match the T-wave segmentation strategy used in the UKB cohort, the T-wave segmentation window was subsequently adjusted by shifting the T-wave boundaries (T_{on} and T_{off}) forward in time by an offset linearly proportional to the RR interval, defined as $T_{on} = QRS_{off} + 40\,\text{ms} \times RR/1000$ and $T_{off} = T_{off} + 40\,\text{ms} \times RR/1000$, where QRS_{off} denotes the end of the QRS complex. Finally, each isolated T wave was further filtered using a sixth-order bidirectional low-pass Butterworth filter with a cutoff frequency of 20 Hz to eliminate residual high-frequency content.

Quantification of T-Wave Morphology Changes

To assess T-wave morphology changes, we used TMV index, a dynamic time-warping–based algorithm previously validated for quantifying morphology changes relative to reference repolarization patterns.[25,28–30] TMV

Downloaded from http://ahajournals.org by on July 6, 2026

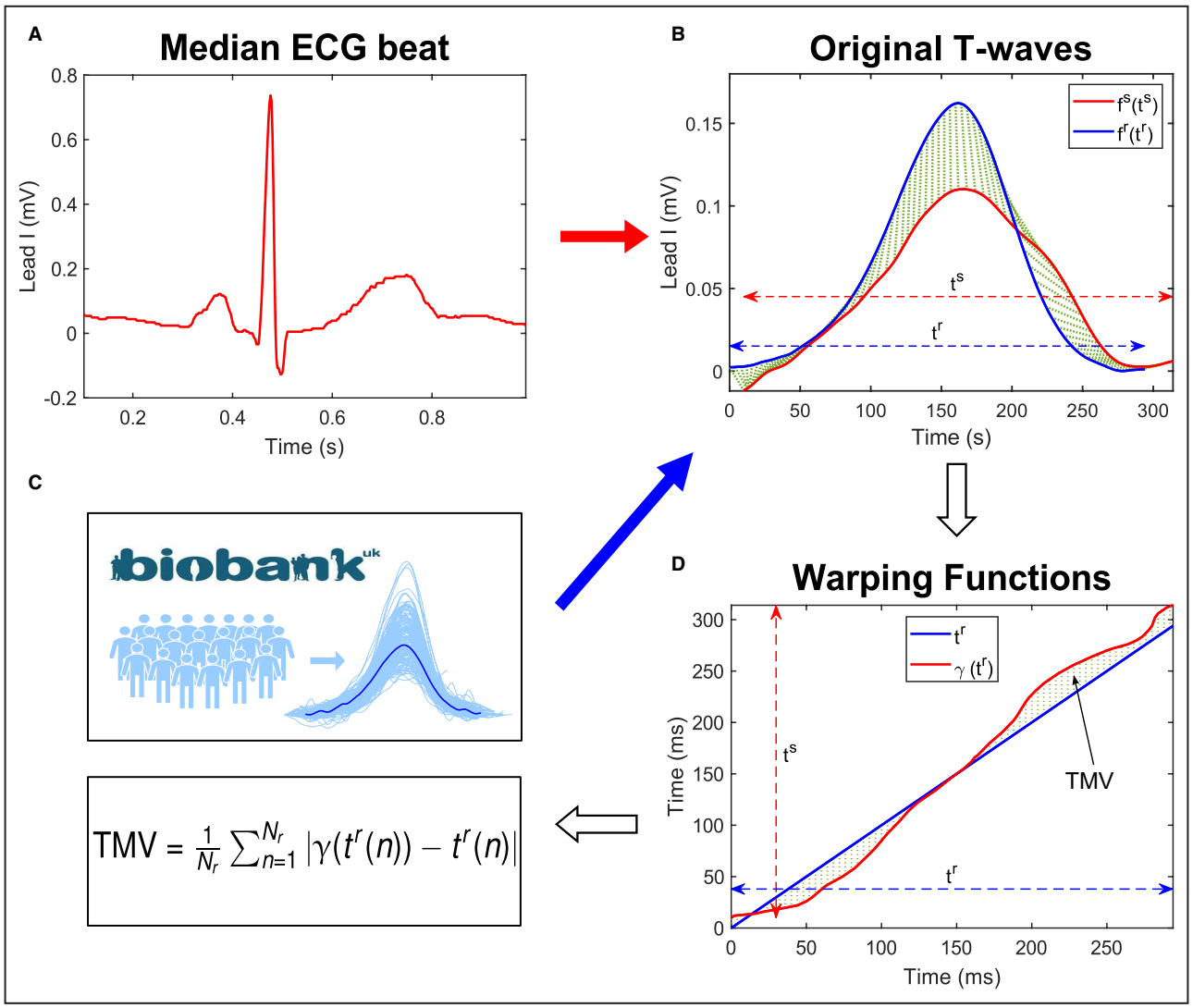


Figure 1. Diagram of the method to obtain the time-warping–based index, TMV.
The color blue across panels corresponds to the healthy general condition, and the red one to LQT2. **A**, Illustrative median ECG beat derived from the 10-second ECG recording in lead I for a particular patient. **B**, A median T wave (red line) extracted from **A** for an individual patient together with its corresponding sex-, heart rate–, and lead-specific normal reference wave (blue line) derived from the UK Biobank cohort represented by **C**. The green dashed lines illustrate temporal pointwise differences that would be necessary to optimally match f^s wave with f^r wave. **D**, Warping function $\gamma(t^r)$ (solid red line) that optimally relates the reference $f^r(t^r)$ and studied $f^s(t^s)$ waves. TMV index representing the total amount of warping is depicted by the green dashed line area between $\gamma(t^r)$ and t^r. LQT2 indicates type 2 long-QT syndrome; and TMV, T-wave morphology variation.

reflects the signed average time warping required to optimally align each point of the T wave under study to a representative normal reference T wave, thus providing a geometry-aware measure of morphologic variation. In brief, each median T wave, derived from each 10-s ECG recording as described above, was compared with its corresponding sex-, heart-rate–, and lead-matched average reference waveform derived from the UKB population cohort (Figure 1C). TMV is defined as follows:

$$\mathrm{TMV} = \frac{1}{N_r}\sum_{n=1}^{N_r}\left|\gamma\left(t^r(n)\right) - t^r(n)\right| \quad (1)$$

where $\gamma(t^r)$ (solid red line in Figure 1D) is the optimal warping function that reparametrizes the time dimension of the patient's T wave to best match its corresponding reference waveform $f^r(t^r)$ (of length N_r), with an additional derivative-based weighting variable that has recently shown improved robustness against noise.[35] TMV is depicted as the average green dashed line area in Figure 1D. TMV is additionally reported as a signed measure, whose sign follows the net amount of warping (see Data S1 for mathematical details). A positive (negative) sign indicates that aligning the wave under study

Downloaded from http://ahajournals.org by on July 6, 2026

with the reference one predominantly requires stretching (shrinking) the waveform, and larger absolute TMV values indicate greater deviation from normal T-wave morphology. Figure 1 summarizes the processing pipeline used to compute the TMV index for each patient. All outcome and risk analyses were performed exclusively in the cohort with LQT2.

Given prior reports linking lower T-wave amplitude with increased arrhythmic risk[16] and showing genotype-dependent, circadian modulation of beat-to-beat T-wave amplitude variability in LQTS,[13] we included a simple amplitude metric derived from each median beat. T-wave amplitude, T_{Amp}, was defined as the absolute difference between the signal amplitude at the automatically annotated T-wave peak (wavelet-based method[34]) and the mean voltage of an isoelectric segment of the same beat. The isoelectric segment was defined as a window of $10\,ms \times RR/1000$ within the PR interval whose end was positioned $15\,ms \times RR/1000$ before QRS onset. If the window extended beyond the PR segment, it was truncated to remain within PR. Similarly, considering prior literature on morphology-based risk markers, we also included the MCS[36] as a benchmark comparator. MCS was obtained from the QT Guard Plus software (GE Healthcare) using each median beat. This algorithm computes MCS from T-wave flatness, asymmetry, and notching, according to the method proposed by Andersen et al.[36] and further explored in subsequent studies.[22,23,37]

To further evaluate the added value of the warping-based index, standard clinical measurements were extracted from each available ECG recording to serve as comparative references. RR and QT intervals were measured in milliseconds, and QT values were corrected for heart rate using the Bazett formula.

The workflow was fully automated (median-beat annotation and TMV computation). Visual inspection of annotated median beats and the TMV graphical output was then performed as a verification step of the automated output (no manual reannotation was required).

Statistical Analysis

All data were first assessed for distributional normality using the Shapiro–Wilk test. Continuous variables are summarized as mean±SD or as median and interquartile range, depending on distribution. Categorical variables are presented as absolute frequencies and percentages. Group comparisons were performed using the Student *t*-test or the Mann–Whitney *U* test for continuous variables, and the χ^2 or Fisher exact test for categorical variables, as appropriate.

To explore the prognostic performance of the TMV index, we dichotomized TMV using the population's 25th percentile as a cutoff value. Kaplan–Meier survival curves were generated to assess cumulative event-free survival, and differences between groups were evaluated using the log-rank test. The association with clinical events was evaluated using Cox proportional hazards regression to estimate hazard ratios (HRs) and 95% CIs for the first lifetime occurrence of age-dependent CE, using age as the time scale[5,38] (birth as time origin), with follow-up censored at the age of 60 years, in line with previous LQTS studies[39,40] and assuming no population-scale changes in the distribution of TMV values throughout the lifespan. Multivariable Cox models adjusted for QTc, sex, and MCS were also performed. The proportional hazards assumption was assessed using standard graphical diagnostics (log-minus-log plots) and time-dependence checks (introduction of a time-dependent covariate into the model). Model discrimination was summarized using Uno's concordance index (C-index) for the Cox models. Model calibration was assessed at time 50 years using internal bootstrap validation with 400 resamples and comparing predicted and observed event risk, and an optimism-corrected calibration to reduce overfitting-related bias from using the same data set for model development and evaluation. β-Blocker therapy was not included in the main multivariable models and was considered only in sensitivity analyses because of its potential confounding effect and time-varying nature. All statistical analyses were 2 tailed and considered significant if $P<0.05$. Analyses were performed using MATLAB R2024b and IBM SPSS Statistics for Windows 29.0.1.0 (IBM Corporation, Armonk, NY).

Additionally, TMV computations were performed offline and blinded to clinical outcomes. Statistical analyses were subsequently conducted independently by the clinical investigators.

RESULTS

Clinical and Demographic Characteristics

A total of 54 patients with congenital LQT2 were included in the study. Table 1 summarizes the demographic variables, baseline ECG intervals (RR, QRS, and QTc), and treatment status up to the age of 60 years. The cohort had a median age at first ECG of 35 years and a balanced sex distribution. At baseline, resting heart rate was in the low-normal range, QRS duration was within normal limits with no evidence of intraventricular conduction delay, and QTc was moderately prolonged with interindividual variability, consistent with the LQT2 phenotype. The vast majority of patients were treated with β-blockers.

Downloaded from http://ahajournals.org by on July 6, 2026

Table 1. Clinical Characteristics of Patients With LQT2

Characteristics	Patients with LQT2 (n=54)
Demographics	
Male, N (%)	25 (45.45)
Age at first ECG, y	35 (21–47)
Age at end of follow-up, y	52 (37–66)
Electrocardiography	
RR, ms	951 (843–1110)
QRS, ms	88 (82–96)
QTc, ms	472 (449–499)
Treatment (up to the age of 60 y), n (%)	
β-Blockers	46 (85)
ICD	15 (28)
Pacemaker	7 (13)
Cardiac events lifelong, n (%)*	32 (58)
Syncope	28 (51)
Documented VA	11 (20)
Cardiac events, before the age of 60 y, n (%)	25 (46)
Of those documented VA	10 (18)

Data are presented as number (percentage) or median (quartile 1–quartile 3). Documented VA included torsades de pointes, ventricular tachycardia, appropriate ICD therapy, aborted cardiac arrest, and sudden cardiac death.

ICD indicates implantable cardioverter-defibrillator; LQT2, type 2 long-QT syndrome; VA, ventricular arrhythmia.

*Syncope and documented VA are not mutually exclusive; patients with both are counted in both rows but only once in cardiac event (≥1 event).

T-Wave Morphology

Analysis of TMV across the 8 independent leads revealed a consistent pattern, with statistical significance emerging in lead I in this cohort. Therefore, we report descriptive ECG-derived metrics and clinical outcome analyses for lead I. The simple amplitude metric, T_{Amp}, showed a median (quartile 1–quartile 3) of 0.17 (0.12–0.23) mV across the cohort. Beyond amplitude, the distribution of the TMV index across patients with LQT2 patients ranged from −32.81 to 24.78 ms, with median (quartile 1–quartile 3) of −12.96 (−18.41 to −7.81) ms. Note that, because the warping indexes are signed, negative values indicate a temporal compression (shrinkage) of the repolarization phase required to align the patient waveform with the reference waveform, reflecting a broader or delayed repolarization phase in the original signal. When comparing by sex, TMV did not differ between men and women, with median (quartile 1–quartile 3) values of −12.64 (−20.27 to −8.12) ms in men and −13.68 (−17.01 to −6.92) ms in women (P=0.808). The cohort's 25th percentile (quartile 1=−18.41 ms) was used as the cutoff to evaluate associations of the TMV index with relevant clinical and electrocardiographic variables.

As summarized in Table 2, demographic profiles were comparable between patients with low TMV and those with higher TMV, with no differences in sex distribution or age at the first ECG. Baseline RR and QRS did not differ between groups, with comparable resting heart rates and uniformly narrow QRS complexes. In contrast, QTc was higher in the subjects with LQT2 with lower TMV. For treatment, β-blocker use did not differ significantly between groups, implantable cardioverter-defibrillator implantation was significantly more frequent in the low-TMV group, whereas pacemaker use was similar in both groups. Among T-wave metrics, the MCS index was significantly higher in the low-TMV group, whereas T_{Amp} index showed no between-group difference.

Association of ECG Markers With Cardiac Outcomes

At least 1 CE occurred in 32 patients; 28 patients had syncope, and 11 had documented VA (categories not mutually exclusive). Neither T_{Amp} nor MCS demonstrated a significant association with the risk of CE (T_{Amp}: HR, 0.53 [95% CI, 0.00–7.10]; P=0.240; MCS: HR, 1.25 [95% CI, 0.67–2.38]; P=0.489). Both analyses yielded wide 95% CIs and concordant nonsignificant results, indicating no predictive value in this cohort.

In contrast, patients with low TMV (≤−18.41 ms) were more likely to experience CEs, either syncope or VA, than those with higher TMV (93% versus 43%; Table 2). Importantly, this pattern remained statistically significant when considering VA alone, as shown by the comparison of VA proportions between groups (43% versus 10%).

Cardiac Events

Figure 2A shows Kaplan–Meier survival curves for time to first CE, comparing patients with LQT2 below the 25th-percentile TMV cutoff (purple line) with the remainder of the cohort (blue line). Patients in the lowest-quartile group exhibited markedly reduced event-free survival compared with the rest of the cohort, with an early and sustained separation of curves. The log-rank test indicated a significant difference between groups (P<0.001). Accordingly, TMV ≤ −18.41 ms was associated with increased risk in the univariate model (HR, 3.505 [95% CI, 1.673–7.341]; P<0.001). In multivariable analyses, the association remained significant after adjustment for QTc and after additional adjustment for sex and MCS. Full multivariable estimates are provided in Table 3, whereas the univariate analysis of the remaining ECG leads in which no significant findings were found is presented in Table S1. Across those leads, TMV showed similar risk estimates, however not reaching statistical significance. Model discrimination for the univariable TMV Cox model was modest (Uno C-index=0.61 [95%

Downloaded from http://ahajournals.org by on July 6, 2026

Table 2. Characteristics of Patients With LQT2 Based on Cutoffs of the 25th Percentile (Quartile 1) of the TMV Index

Characteristics	TMV≤quartile 1	TMV>quartile 1	*P* value
No.	14	40	
Demographics			
Male, N (%)	7 (50)	18 (45)	0.762
Age at first ECG, y	28 (18–44)	37 (24–51)	0.235
Electrocardiography			
RR, ms	951 (819–1112)	950 (866–1098)	0.569
QRS, ms	88 (82–90)	88 (82–97)	0.504
QTc, ms	508 (498–517)	463 (442–480)	0.003*
T wave			
MCS	1.89±0.58	1.24±0.41	<0.001*
T_{Amp}, mV	0.16±0.05	0.18±0.08	0.413
Treatment, up to the age of 60 y, n (%)			
β-Blockers	14 (100)	31 (78)	0.092
ICD	8 (57)	7 (18)	0.012*
Pacemaker	2 (14)	5 (13)	1.000
Cardiac events lifelong, n (%)†	13 (93)	19 (48)	0.004*
Syncope	11 (79)	17 (43)	0.030*
Documented VA	6 (43)	5 (13)	0.024*
Cardiac events, before the age of 60 y	13 (93)	17 (43)	0.001*
Of those documented VA	6 (43)	4 (10)	0.013*

In this cohort, quartile 1 (25th percentile) of TMV corresponds to –18.41 ms. Data are presented as number (percentage), mean±SD, or median (quartile 1–quartile 3). Documented VA included torsades de pointes, ventricular tachycardia, appropriate ICD therapy, aborted cardiac arrest, and sudden cardiac death.

ICD indicates implantable cardioverter-defibrillator; LQT2, type 2 long-QT syndrome; MCS, morphology combination score; T_{Amp}, T-wave amplitude; TMV, T-wave morphology variation; and VA, ventricular arrhythmia.

*Values indicate significance, $P<0.05$.

†Syncope and documented VA are not mutually exclusive; patients with both are counted in both rows but only once in cardiac event (≥1 event).

CI, 0.533–0.693]) and increased slightly in the fully adjusted model (TMV+QTc+sex+MCS; Uno C-index=0.65 [95% CI, 0.539–0.754]). Internal bootstrap calibration suggested reasonable agreement between predicted and observed risk at the 50-year time horizon after optimism correction. The mean absolute calibration error was 4.3%, with higher deviation at the extremes.

As a sensitivity analysis, we additionally included β-blocker therapy in the fully adjusted model (TMV+QTc+sex+MCS) and the association remained significant (HR, 4.137 [95% CI, 1.405–12.183]; *P*=0.010).

Ventricular Arrhythmias

Figure 2B shows the Kaplan–Meier curve for time to first VA, where the TMV ≤ –18.41 ms group also had lower VA-free survival, with a similar early divergence maintained across the recorded clinical history (log-rank *P*=0.006). In the univariate Cox model, low TMV (≤–18.41 ms) was associated with increased risk of VA (HR, 4.978 [95% CI, 1.4–17.705]; *P*=0.013). In multivariable models, estimates were directionally similar but did not reach statistical significance: adjusted HRs ranged from 2.623 to 3.116, but all 95% CIs crossed 1.0 (smallest *P*=0.164). Corresponding HRs and 95% CIs are reported in Table 3.

DISCUSSION

The present study assesses the association of the TMV index with CEs in patients with LQT2. Changes in T-wave morphology in each of the 8 independent leads were quantified by means of a time-warping–based method that quantifies morphologic variations with respect to a healthy population-based reference T wave. Our main findings are that the TMV index in lead I was significantly associated with an increased risk of CEs in patients with LQT2. More negative values of TMV index, reflecting broader T waves and greater morphologic dissimilarity from the normal T-wave pattern, were linked to the occurrence of CE after adjustment for QTc prolongation, and the association remained significant in models further adjusted for sex and MCS, a T-wave morphology index earlier studied in the context of type 2 LQTS or interventions involving I_{Kr} (human ether-à-go-go-related gene, hERG) channel inhibition. When ventricular arrhythmia was considered

Downloaded from http://ahajournals.org by on July 6, 2026

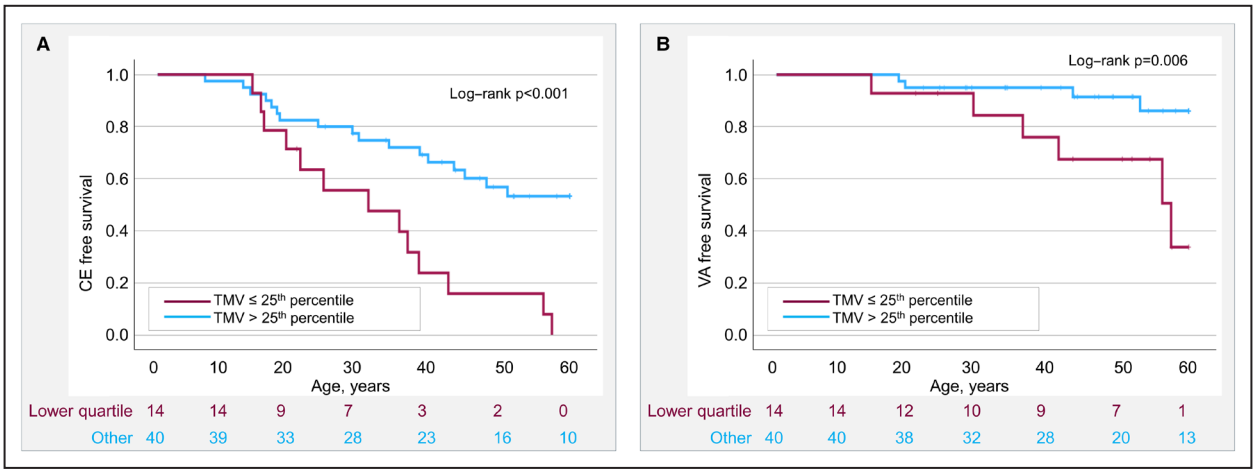


Figure 2. Probability of CE-free survival over lifetime censored at the age of 60 years in patients with LQT2 dichotomized by the 25th percentile cutoff of the lead I–derived TMV index: time to first cardiac event (A) and time to first ventricular arrhythmia (B).

CE indicates cardiac event; LQT2, type 2 long-QT syndrome; TMV, T-wave morphology variation; and VA, ventricular arrhythmia.

Downloaded from http://ahajournals.org by on July 6, 2026

as the end point, the association was significant in the univariate model but did not persist after multivariable adjustment.

Although many studies have explored T-wave morphology in LQTS, only a few have successfully provided prognostic information beyond subtype classification or comparison with healthy controls. Among them, visually assessed abnormalities, such as flat or notched T waves, have shown associations with increased cardiac risk in LQT2 carriers with normal QTc.[18] A more quantitative approach was proposed by Sugrue et al, who identified the T-wave center of gravity x axis in lead I (computed over the last 25% of the wave) as an independent predictor of breakthrough CEs in patients with LQT2, showing prognostic value beyond QTc in that subgroup.[41] In line with this lead-dependent pattern, TMV association with CEs emerged in lead I, whereas other leads did not reach statistical significance (Table S1), suggesting that repolarization vector alignment and cohort-specific factors influence lead-specific detectability. In addition, this concordance with lead I may reflect that TMV, although computed over the full T wave, can be dominated by late or terminal repolarization mismatches relative to the reference, and may therefore capture tail-weighted integral properties of the T wave, as summarized by the lead-I center-of-gravity metric. More recently, the 3-dimensional T-wave vector magnitude has been shown to identify high-risk LQT2 mutation carriers with normal QTc.[16] Most of these approaches are constrained to subsets of patients without QT prolongation. In contrast, our approach is the first to apply a warping-based method to this context, capturing subtle morphologic variations across the full T wave and showing an association with higher risk in patients with LQT2 that is independent of QTc duration. Specifically, we applied a single TMV cutoff (≤–18.41 ms) to categorize patients in this cohort, which captured the most pronounced T-wave morphologic changes associated with increased risk.

Table 3. Risk of CEs and VAs in Patients With LQT2: Cox Regression Analysis Dichotomized by the 25th Percentile of the TMV Index Derived From Lead I

Adjustment	HR	95% CI	*P* value
CEs			
QTc	2.92	1.111–7.676	0.03*
QTc and sex	3.375	1.256–9.067	0.016*
QTc, sex, and MCS	4.061	1.369–12.046	0.012*
VAs			
QTc	3.035	0.625–14.728	0.168
QTc and sex	3.116	0.629–15.430	0.164

CE indicates cardiac event; HR, hazard ratio; LQT2, type 2 long-QT syndrome; MCS, morphology combination score; QTc, corrected QT; TMV, T-wave morphology variation; and VA, ventricular arrhythmia.

*Values indicate significance, $P<0.05$.

Survival analysis revealed a consistent trend: patients with wider T waves and more pronounced T-wave morphologic changes, as indicated by more negative TMV values, had significantly lower event-free survival compared with the rest of the cohort, reflecting a higher vulnerability to CEs when the T-wave morphology differs largely from the normal pattern. Moreover, Cox regression analyses point to the same risk profile, further supporting the consistency of the TMV index. The association persisted after adjustment for QTc, suggesting that TMV captures relevant information not fully conveyed by QTc prolongation alone. The association persisted after adjustment for sex and remained significant with additional adjustment for MCS,

indicating that TMV provides additional information not conveyed by these covariates.

Although MCS values were significantly higher in the low-TMV group (Table 2), indicating morphologic abnormalities that covary with TMV, MCS itself was not associated with CEs in this cohort. This pattern suggests that between-group contrasts can arise from correlated morphology features without translating into independent prognostic signal at the patient level. In other words, MCS appears to track with TMV cross-sectionally but does not carry sufficient information to inform risk on its own in this cohort, likely reflecting a smaller effect size and lower sensitivity of MCS, which would require a larger cohort to detect its association with outcomes. By contrast, TMV remained associated with outcomes after multivariable adjustment, MCS included, indicating that TMV captures the information not included in MCS. Conceptually, the warping-based approach may better summarize temporally dispersed repolarization changes that are less accessible to composite asymmetry/notch/flatness aggregates. Separately, T-wave amplitude values were overall low across the cohort, consistent with the low-amplitude T-wave phenotype often described in LQT2. However, associations with CEs were consistently nonsignificant, indicating limited precision that may reflect the small sample size. Taken together with the TMV results, these findings suggest that neither T_{Amp} nor MCS had discriminant value here, whereas a full-T-wave, warping-based measure captured morphology information relevant to risk in LQT2 within our data set.

A plausible mechanistic rationale for the observed findings is that loss of function of the rapid delayed rectifier potassium current (I_{Kr}) from *KCNH2* mutations amplifies temporal and spatial heterogeneity of repolarization, manifesting as T-wave morphology changes. Such changes may not be fully captured by QTc duration alone. By applying a full-T-wave, morphology-aware alignment, as provided by the warping-based strategy, the TMV index quantifies pointwise timing variations relative to a population reference and thereby reflects broader or temporally dispersed repolarization patterns characteristic of LQT2. This provides a concise morphologic summary that complements the QTc and helps to discriminate patients with significantly lower event-free survival within this genotype, including those with borderline or moderately prolonged QTc.

A possible explanation for the lack of statistical significance in the adjusted models for VA is the limited number of events available for analysis (10 events before the age of 60 years), which reduces statistical power and inflates 95% CIs. The inclusion of prespecified covariates (QTc, sex, and MCS) may also have attenuated estimates by distributing shared prognostic information. Further confirmation in larger cohorts, containing more VA events, will be essential in subsequent studies.

Although the role of sex in modulating arrhythmic risk among patients with LQT2 has previously been suggested by Cortez et al, who reported that abnormal T-wave morphology conferred higher risk in women with normal QTc but not in men,[16] Sugrue et al did not report sex-stratified results in their analysis of morphology-based ECG markers in a size-comparable cohort.[41] In our study, TMV distributions did not differ by sex (Table 2), suggesting a relatively homogeneous morphologic substrate between men and women. Moreover, including sex as a covariate did not alter the association between TMV and CEs, indicating that the prognostic value of TMV was independent of sex in our models. We did not perform sex-specific risk analyses because of the limited cohort size and number of events, so these observations should be interpreted with caution and more robustly evaluated in larger, sex-balanced cohorts.

Despite extensive explorations of ECG metrics to refine risk stratification in LQTS, progress toward routine use of morphology-based markers has been limited by variability in measurement protocols and challenges in validation and standardization. Within this context, TMV offers a single-lead measure of full T-wave morphologic variations relative to a large and consistent population template, thereby facilitating straightforward large-scale comparison with normal patterns and enabling prespecified dichotomization for clinical analyses. From a clinical perspective, TMV may serve as a valuable complement to existing risk stratification tools in patients with LQT2, including those with borderline or prolonged QTc values. As TMV index is computable directly from T-wave morphology and does not rely on specific fiducial points, it may be well suited for automated implementation in digital ECG platforms. Future studies should aim to validate these findings in larger, prospective cohorts and evaluate whether warping-index–based classification improves clinical decision-making or risk prediction models.

Limitations

This study has limitations that should be acknowledged. First, this single-cohort study has a retrospective nature and is intended as exploratory (hypothesis generating); therefore, the findings should be interpreted accordingly. Second, the overall LQT2 cohort size was limited, which restricted the ability to perform subgroup risk analyses and may have reduced power to detect weak associations. Accordingly, stratified analyses by sex or by QTc interval range (eg, normal versus prolonged) were not conducted because of the relatively low number of events across both groups. Thus, no formal sex-related risk interaction analysis was performed either. In

Downloaded from http://ahajournals.org by on July 6, 2026

addition, the high concentration of events in the lowest TMV quartile leaves few event-free individuals in that stratum, which may reduce the stability of adjusted estimates and contribute to wide 95% CIs. Consequently, validation in a larger cohort is needed to confirm its clinical utility and generalizability and to enable a robust assessment of model performance (including discrimination and calibration).

CONCLUSIONS

T-wave morphology abnormalities quantified by the TMV index showed a statistically significant association with the risk of CEs in a cohort of patients with LQT2, which included those with prolonged or borderline QTc values, after adjustment for QTc, sex, and MCS. These markers reflect repolarization abnormalities not captured by QTc duration and may complement current risk stratification strategies. Further validation in prospective, multicenter cohorts is warranted to support their potential integration into clinical practice.

ARTICLE INFORMATION

Received December 3, 2025; accepted May 12, 2026.

Affiliations

Aragón Institute of Engineering Research, IIS Aragón, University of Zaragoza, Zaragoza, Spain (N.G., J.R., J.P.M., P.L.); Centro de Investigación Biomédica en Red–Bioingeniería, Biomateriales y Nanomedicina, Zaragoza, Spain (N.G., J.R., J.P.M., P.L.); William Harvey Research Institute, Queen Mary University of London, London, UK (J.R.); Department of Cardiology, Clinical Sciences, Lund University, Lund, Sweden (A.A.S., U.C., P.G.P.); Department of Cardiology, Sahlgrenska University Hospital, Gothenburg, Sweden (P.D.); Department of Cardiology and Department of Health, Medicine and Caring Sciences, Linkoping University, Linköping, Sweden (A.S.); Department of Clinical Genetics, University and Regional Laboratories, Lund University Hospital, Lund University, Lund, Sweden (N.L.); and Arrhythmia Clinic, Skåne University Hospital Lund, Lund, Sweden (E.L., U.C., P.G.P.).

Sources of Funding

Funding was provided by the Ministry of Science, Innovation and Universities, Spain, projects: PID2022-140556OB-I00, PID2023-148975OB-I00, and CNS2023-143599, and by Aragón Government group: Biomedical Signal Interpretation and Computational Simulation T39_23R. P.P. was supported by the Swedish Heart Lung Foundation (2023–2025), grants from the Swedish state under the agreement between the Swedish government and the county councils (the ALF agreement), and donation funds at Skåne University Hospital. Computations were performed at the High-Performance Computing unit of NANBIOSIS, a Spanish Singular Scientific and Technical Infrastructure.

Disclosures

None.

Supplemental Material

Data S1. Supplemental Methods
Table S1

REFERENCES

1. Schwartz PJ, Stramba-Badiale M, Crotti L, Pedrazzini M, Besana A, Bosi G, Gabbarini F, Goulene K, Insolia R, Mannarino S, et al. Prevalence of the congenital long-QT syndrome. *Circulation*. 2009;120:1761–1767. doi: 10.1161/CIRCULATIONAHA.109.863209
2. Crotti L, Celano G, Dagradi F, Schwartz PJ. Congenital long QT syndrome. *JACC Clin Electrophysiol*. 2022;8:687–706. doi: 10.1016/j.jacep.2022.02.017
3. Rieder M, Kreifels P, Stuplich J, Ziupa D, Servatius H, Nicolai L, Castiglione A, Zweier C, Asatryan B, Odening KE. Genotype-specific ECG-based risk stratification approaches in patients with long-QT syndrome. *Front Cardiovasc Med*. 2022;9:916036. doi: 10.3389/fcvm.2022.916036
4. Schwartz PJ, Crotti L, Insolia R. Long-QT syndrome. *Circ Arrhythm Electrophysiol*. 2012;5:868–877. doi: 10.1161/CIRCEP.111.962019
5. Goldenberg I, Horr S, Moss AJ, Lopes CM, Barsheshet A, S MN, Zareba W, Andrews ML, Robinson JL, Locati EH, et al. Risk for life-threatening cardiac events in patients with genotype-confirmed long-QT syndrome and normal-range corrected QT intervals. *JACC*. 2011;57:51–59. doi: 10.1016/j.jacc.2010.07.038
6. Zareba W, Cygankiewicz I. Long QT syndrome and short QT syndrome. *Prog Cardiovasc Dis*. 2008;51:264–278. doi: 10.1016/j.pcad.2008.10.006
7. Goldenberg I, Moss AJ. Long QT syndrome. *J Am Coll Cardiol*. 2008;51:2291–2300. doi: 10.1016/j.jacc.2008.02.068
8. Srutova M, Kremen V, Lhotska L. Electrocardiographic discrimination of long QT syndrome genotypes: a comparative analysis and machine learning approach. *Sensors*. 2025;25:2253. doi: 10.3390/s25072253
9. Abrams DJ, MacRae CA. Long QT syndrome. *Circulation*. 2014;129:1524–1529. doi: 10.1161/CIRCULATIONAHA.113.003985
10. Sugrue A, Noseworthy PA, Kremen V, Bos JM, Qiang B, Rohatgi RK, Sapir Y, Attia ZI, Brady P, Asirvatham SJ, et al. Identification of concealed and manifest long QT syndrome using a novel T wave analysis program. *Circ Arrhythm Electrophysiol*. 2016;9:e003830. doi: 10.1161/CIRCEP.115.003830
11. Immanuel SA, Sadrieh A, Baumert M, Couderc JP, Zareba W, Hill AP, Vandenberg JI. T-wave morphology can distinguish healthy controls from LQTS patients. *Physiol Meas*. 2016;37:1456–1473. doi: 10.1088/0967-3334/37/9/1456
12. Sy RW, van der Werf C, Chattha IS, Chockalingam P, Adler A, Healey JS, Perrin M, Gollob MH, Skanes AC, Yee R, et al. Derivation and validation of a simple exercise-based algorithm for prediction of genetic testing in relatives of LQTS probands. *Circulation*. 2011;124:2187–2194. doi: 10.1161/CIRCULATIONAHA.111.028258
13. Extramiana F, Tatar C, Maison-Blanche P, Denjoy I, Messali A, Dejode P, Iserin F, Leenhardt A. Beat-to-beat T-wave amplitude variability in the long QT syndrome. *Europace*. 2010;12:1302–1307. doi: 10.1093/europace/euq137
14. Akar FG, Yan G-X, Antzelevitch C, Rosenbaum DS. Unique topographical distribution of M cells underlies reentrant mechanism of torsade de pointes in the long-QT syndrome. *Circulation*. 2002;105:1247–1253. doi: 10.1161/hc1002.105231
15. Lang CN, Menza M, Jochem S, Franke G, Perez Feliz S, Brunner M, Koren G, Zehender M, Bugger H, Jung BA, et al. Electro-mechanical dysfunction in long QT syndrome: role for arrhythmogenic risk prediction and modulation by sex and sex hormones. *Prog Biophys Mol Biol*. 2016;120:255–269. doi: 10.1016/J.PBIOMOLBIO.2015.12.010
16. Cortez D, Zareba W, McNitt S, Polonsky B, Rosero SZ, Platonov PG. Quantitative T-wave morphology assessment from surface ECG is linked with cardiac events risk in genotype-positive KCNH2 mutation carriers with normal QTc values. *J Cardiovasc Electrophysiol*. 2019;30:2907–2913. doi: 10.1111/jce.14210
17. Tardo DT, Peck M, Subbiah RN, Vandenberg JI, Hill Adam P. The diagnostic role of T wave morphology biomarkers in congenital and acquired long QT syndrome: a systematic review. *Ann Noninvasive Electrocardiol*. 2023;28:e13015. doi: 10.1111/anec.13015
18. Platonov PG, McNitt S, Polonsky B, Rosero SZ, Kutyifa V, Huang A, Moss AJ, Zareba W. Risk stratification of type 2 long-QT syndrome mutation carriers with Normal QTc interval. *Circ Arrhythm Electrophysiol*. 2018;11:e005918. doi: 10.1161/CIRCEP.117.005918
19. Moss AJ, Zareba W, Benhorin J, Locati EH, Hall WJ, Robinson JL, Schwartz PJ, Towbin JA, Vincent GM, Lehmann MH, et al. ECG T-wave patterns in genetically distinct forms of the hereditary long QT syndrome. *Circulation*. 1995;92:2929–2934. doi: 10.1161/01.CIR.92.10.2929
20. Couderc JP, Xia X, Peterson DR, McNitt S, Zhao H, Polonsky S, Moss AJ, Zareba W. T-wave morphology abnormalities in benign, potent, and

Downloaded from http://ahajournals.org by on July 6, 2026

arrhythmogenic Ikr inhibition. *Heart Rhythm*. 2011;8:1036–1043. doi: 10.1016/J.HRTHM.2011.02.005
21. Vaglio M, Couderc JP, McNitt S, Xia X, Moss AJ, Zareba W. A quantitative assessment of T-wave morphology in LQT1, LQT2, and healthy individuals based on Holter recording technology. *Heart Rhythm*. 2008;5:11–18. doi: 10.1016/J.HRTHM.2007.08.026
22. Graff C, Struijk JJ, Matz J, Kanters JK, Andersen MP, Nielsen J, Toft E. Covariate analysis of QTc and T-wave morphology: new possibilities in the evaluation of drugs that affect cardiac repolarization. *Clin Pharmacol Ther*. 2010;88:88–94. doi: 10.1038/clpt.2010.51
23. Graff C, Andersen MP, Xue JQ, Hardahl TB, Kanters JK, Toft E, Christiansen M, Jensen HK, Struijk JJ. Identifying drug-induced repolarization abnormalities from distinct ECG patterns in congenital long QT syndrome. *Drug Saf*. 2009;32:599–611. doi: 10.2165/00002018-200932070-00006
24. Hermans BJM, Stoks J, Bennis FC, Vink AS, Garde A, Wilde AAM, Pison L, Postema PG, Delhaas T. Support vector machine-based assessment of the T-wave morphology improves long QT syndrome diagnosis. *EP Europace*. 2018;20:iii113–iii119. doi: 10.1093/europace/euy243
25. Ramírez J, Orini M, Tucker JD, Pueyo E, Laguna P. Variability of ventricular repolarization dispersion quantified by time-warping the morphology of the T-waves. *IEEE Trans Biomed Eng*. 2017;64:1619–1630. doi: 10.1109/TBME.2016.2614899
26. Ramírez J, Orini M, Mincholé A, Monasterio V, Cygankiewicz I, Bayés de Luna A, Martínez JP, Pueyo E, Laguna P. T-wave morphology restitution predicts sudden cardiac death in patients with chronic heart failure. *J Am Heart Assoc*. 2017;6:e005310. doi: 10.1161/JAHA.116.005310
27. Ramírez J, van Duijvenboden S, Aung N, Laguna P, Pueyo E, Tinker A, Lambiase PD, Orini M, Munroe PB. Cardiovascular predictive value and genetic basis of ventricular repolarization dynamics. *Circ Arrhythm Electrophysiol*. 2019;12:e007549. doi: 10.1161/CIRCEP.119.007549
28. Gómez N, Ramírez J, Martínez JP, Laguna P. Time-warping analysis of the T-wave peak-to-end interval to quantify ventricular repolarization dispersion during ischemia. *IEEE J Biomed Health Inform*. 2023;27:5314–5325. doi: 10.1109/JBHI.2023.3310878
29. Gómez N, Ramírez J, Martín-Yebra A, Demidova MM, Platonov P, Martínez JP, Laguna P. T-wave peak-to-end changes quantified by time-warping predicts ventricular fibrillation in a porcine myocardial infarction model. *IEEE Trans Biomed Eng*. 2024;71:2968–2977. doi: 10.1109/TBME.2024.3404254
30. Ramírez J, Kiviniemi A, van Duijvenboden S, Tinker A, Lambiase PD, Junttila J, Perkiömäki JS, Huikuri HV, Orini M, Munroe PB. ECG T-wave morphologic variations predict ventricular arrhythmic risk in low- and moderate-risk populations. *J Am Heart Assoc*. 2022;11:e025897. doi: 10.1161/JAHA.121.025897
31. Sudlow C, Gallacher J, Allen N, Beral V, Burton P, Danesh J, Downey P, Elliott P, Green J, Landray M, et al. UK biobank: an open access resource for identifying the causes of a wide range of complex diseases of middle and old age. *PLoS Med*. 2015;12:e1001779. doi: 10.1371/journal.pmed.1001779
32. Harris PA, Taylor R, Thielke R, Payne J, Gonzalez N, Conde JG. Research electronic data capture (REDCap)—a metadata-driven methodology and workflow process for providing translational research informatics support. *J Biomed Inform*. 2009;42:377–381. doi: 10.1016/j.jbi.2008.08.010
33. Harris PA, Taylor R, Minor BL, Elliott V, Fernandez M, O'Neal L, McLeod L, Delacqua G, Delacqua F, Kirby J, et al. The REDCap consortium: building an international community of software platform partners. *J Biomed Inform*. 2019;95:103208. doi: 10.1016/j.jbi.2019.103208
34. Martinez JP, Almeida R, Olmos S, Rocha AP, Laguna P. A wavelet-based ECG delineator: evaluation on standard databases. *IEEE Trans Biomed Eng*. 2004;51:570–581. doi: 10.1109/TBME.2003.821031
35. Palmieri F, Gomis P, Ferreira D, Pueyo E, Martínez JP, Laguna P, Ramirez J. Weighted time warping improves T-wave morphology markers clinical significance. *IEEE Trans Biomed Eng*. 2022;69:2787–2796. doi: 10.1109/TBME.2022.3153791
36. Andersen MP, Xue JQ, Graff C, Hardahl TB, Toft E, Kanters JK, Christiansen M, Jensen HK, Struijk JJ. A robust method for quantification of IKr-related T-wave morphology abnormalities. *Comput Cardiol*. 2007;34: 341–344. doi: 10.1109/CIC.2007.4745491
37. Porta-Sánchez A, Spillane DR, Harris L, Xue J, Dorsey P, Care M, Chauhan V, Gollob MH, Spears DA. T-wave morphology analysis in congenital long QT syndrome discriminates patients from healthy individuals. *JACC Clin Electrophysiol*. 2017;3:374–381. doi: 10.1016/J.JACEP.2016.10.013
38. Locati EH, Zareba W, Moss AJ, Schwartz PJ, Vincent GM, Lehmann MH, Towbin JA, Priori SG, Napolitano C, Robinson JL, et al. Age- and sex-related differences in clinical manifestations in patients with congenital long-QT syndrome. *Circulation*. 1998;97:2237–2244. doi: 10.1161/01.CIR.97.22.2237
39. Goldenberg I, Moss AJ, Bradley J, Polonsky S, Peterson DR, McNitt S, Zareba W, Andrews ML, Robinson JL, Ackerman MJ, et al. Long-QT syndrome after age 40. *Circulation*. 2008;117:2192–2201. doi: 10.1161/CIRCULATIONAHA.107.729368
40. Goldenberg I, Bos JM, Yoruk A, Chen AY, Lopes C, Huang DT, Kutyifa V, Younis A, Aktas MK, Z. Rosero S, et al. Risk prediction in women with congenital long QT syndrome. *J Am Heart Assoc*. 2021;10:e021088. doi: 10.1161/JAHA.121.021088
41. Sugrue A, Rohatgi RK, Noseworthy PA, Kremen V, Bos JM, Qiang B, Sapir Y, Attia ZI, Scott CG, Brady P, et al. Architectural T-wave analysis and identification of on-therapy breakthrough arrhythmic risk in type 1 and type 2 long-QT syndrome. *Circ Arrhythm Electrophysiol*. 2017;10:e005648. doi: 10.1161/CIRCEP.117.005648

Downloaded from http://ahajournals.org by on July 6, 2026